RF PROPERTIES OF NON EVAPORABLE GETTER COATINGS IN THE SUB THz RANGE

M. Dehler*, A. Citterio, R. Ganter, Paul Scherrer Institute, Villigen, Switzerland
X. Liu, Institute of High Energy Physics, Beijing, China
C. Hauser, Hamburg University, Hamburg, Germany
S. Alberti, J. Genoud, École Polytechnique Fédérale de Lausanne, Lausanne, Switzerland

Abstract

We report on the measurement of the surface impedance of thin sub-micron non-evaporable getter (NEG) coatings on a copper substrate, as used for distributed pumping in the vacuum system of the Swiss Light Source upgrade (SLS 2.0). Given the low electrical conductivity of NEG, a sub micron thickness with well known properties is required to avoid heat up and beam instabilities. Measurement frequencies of 100 GHz and above are required to obtain a good measurement sensitivity for these ultra-thin coatings. Two quasi-optical test stands were designed for frequencies around 100 and 170 GHz, based on an asymmetric Fabry Perot with spherical feed mirrors coupling to standard waveguides and planar probe mirrors whose surface is to be characterized. 3D printing allowed to produce the feed mirrors together with the RF coupler and waveguide flanges in one integral part, which required only minimal additional processing. The surface impedance of a NEG coated probe is computed by comparing the Q factor of the resonance with that obtained from reference probes fabricated from bulk stainless steel and copper.

INTRODUCTION

Non-evaporable getter (NEG) coatings, typically ternary alloys composed of titanium, zirconium and vanadium, have several attractive properties [1–3]:

A strongly reduced secondary electron yield helps suppressing multipactor effects in RF cavities and other devices. After heat activation, NEG surfaces absorb and store gas molecules, which results in a distributed pumping effect for vacuum devices and obviating the need for external vacuum pumps. For geometries with small apertures and a corresponding low conductance, these are actually the only option to reach ultra low pressures.

We also see a strong reduction of electron (ESD) and photon stimulated (PSD) gas desorption effects. While the ESD properties are attractive for vacuum electronic devices like klystrons to maintain low vacuum pressures, reduced photon stimulated desorption is an important for ring type electron accelerators, where we have high levels of X-ray synchrotron radiation.

The interest in NEG stems from the upgrade of the Swiss Light Source, SLS 2.0 [4–6]. It features a factor 40 improvement of the emittance by a state of the art design using small aperture magnets. The required small diameter vacuum chambers (18-21 mm) pose two interrelated challenges. The first is the vacuum pressure. Scattering between the electrons of the beam and the rest gas affects the beam lifetime and can create instabilities. Pressures below 10^{-9} mbar are required in the presence of the PSD effects, the low pumping conductance of the chamber makes the use of NEG coatings mandatory.

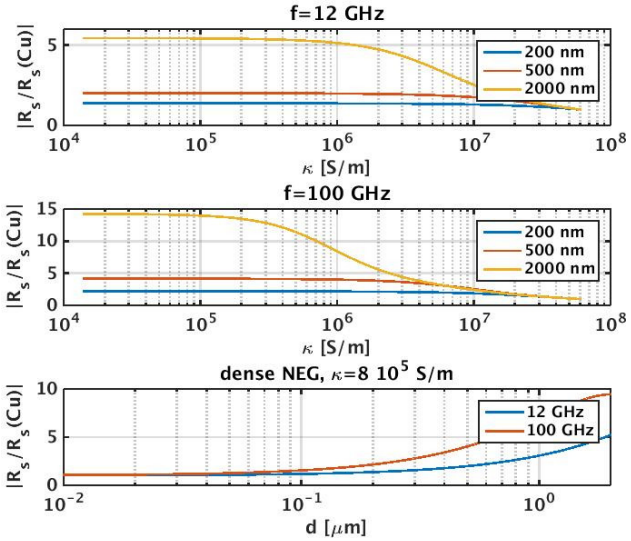

Figure 1: Surface resistance versus coating thickness and frequency. Coatings in the sub micron range require frequencies of 100 GHz and above to be detectable.

The rather high beam current of 400 mA and the wide beam spectrum up to 10 GHz (extending even further for certain kinds of instabilities) makes the surface conductivity of the chamber wall a critical parameter. Depending on the morphology, columnar or dense, bulk type NEG has conductivities between $1.4 \cdot 10^4$ and $8 \cdot 10^5$ S/m [7], very low compared to copper (the bulk material of the chamber) of $5.8 \cdot 10^7$ S/m. Due to the skin effect, the NEG coating dominates the surface impedance at high frequencies with the transition frequency given by the layer thickness. Therefore, to avoid any beam degradation due to resistive wall effects, we use ultra-thin coatings of 500 nm assuming a dense morphology.

Generic measurements of the conductivity of NEG and NEG coatings have already been performed at 7.8 GHz [7] and between 220 and 750 GHz [8]. Both types of measurement require specially prepared samples, an approach not suitable in our case, since we want to be able to use process samples from the actual fabrication.

* micha.dehler@psi.ch

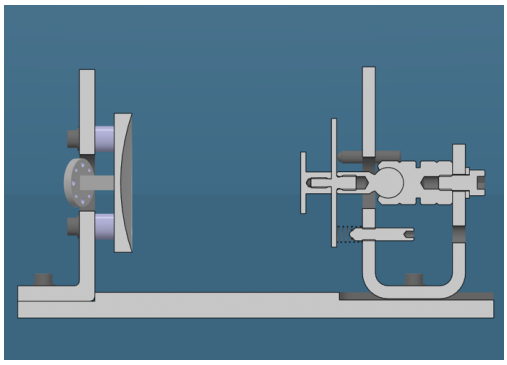

Figure 2: Half Symmetric Fabry Perot.

To test the coating process with respect to the morphology generated, an earlier test run used WR90 waveguides with a relatively thick NEG coating and converted these into resonators in the X band by electrically shortening the ends [9]. This proved the NEG to be of a dense morphology with $\kappa = 8 \cdot 10^5$ S/m. At X band, the skin depth in a NEG layer is above a micron (Fig. 1), the sub micron coatings as used in SLS 2.0 are transparent and measurement frequencies of 100 GHz and more are required for characterization.

THE MEASUREMENT SETUP

In the millimeter region, quasi-optical resonators in the form of Fabry-Perots have been successfully used to measure lossy surfaces [10, 11]. Our design uses the symmetric half of a classic Fabry-Perot, where the large mirror, fabricated from copper, connects to a pair of mutually tilted waveguides (WR 10 for the 100 GHz setup, WR 6.5 for the 170 GHz version) and the sample to be measured, a planar mirror, sits in the symmetry plane (Fig. 2). The transmission between the two waveguides gives the quality factor of the resonance, which itself is a function of the conduction losses on the sample surface.

The complex geometry of the main spherical feed mirror with its two tilted couplers were fabricated with a 3D printing process using an AlSi10Mg alloy. In a second step, the connection surface of the waveguide ports was polished and threads were added to connect the waveguides. A final coating with copper optimized the surface conductivity and smoothed the surface roughness of the mirror. Figure 3 gives a detailed view of the mirror.

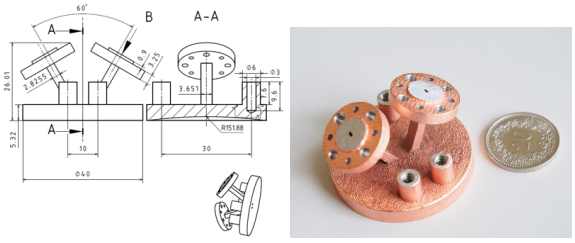

Figure 3: Drawing and photo of spherical mirror at 170 GHz.

Figure 4 shows the field distribution of one of the resonances, the $TEM_{0,0,38}$ mode in the 100 GHz setup. The planar probe mirror, which is our NEG sample, sits in the waist of the Gaussian beam. At a diameter of 24 mm, it is small enough to be introduced into the coating facility as a sample and to be coated together with a normal chamber. Table 1 gives the specification of the Fabry-Perot. The simulations were performed with the TLM solver of CST Studio (for more information, see [9])

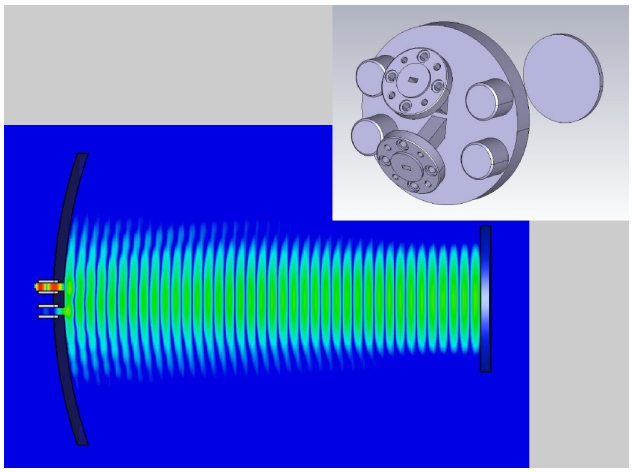

Figure 4: Absolute electrical field amplitude of the $TEM_{0,0,38}$ resonance in the 100 GHz Fabry-Perot between the spherical mirror with integrated couplers (left) and the coated planar sample mirror (right).

The difference between simulated and measured quality factor for the copper probe in Table 1 are due to differences between the simulation model and the mechanical realization. Due to restrictions in CST, the design assumes straight, non-tilted waveguide couplers introducing a certain error. In addition, iris dimensions for the 3D printing process were set so that we would be able to correct coupling by opening up by re-machining the iris apertures. Finally, the subsequent copper coating, also reduced somewhat the apertures of the coupling iris. As it turned out, the reduction in aperture and in coupling was manageable without re-machining, the larger Q even helps to improve the sensitivity of the device.

Table 1: Mechanical and electrical specifications. Simulated Q factors as derived from S parameter calculation.

	100 GHz	**170 GHz**
Curvature feed [mm]	83.7	151.88
⌀ feed [mm]	48.0	40
⌀ probe [mm]	24	24
distance feed/probe [λ]	20	20
RF Coupling	WR10	WR6.5
Simulated Q, all bulk Cu	8490	23642
Measured Q, all bulk Cu	17000	28184

RESULTS

The following methodology for the measurements was used. The total quality factor Q_t of such a setup is determined by the two quality factors Q_e and Q_{rw}

$$\frac{1}{Q_t} = \frac{1}{Q_e} + \frac{1}{Q_{rw}} \quad (1)$$

Q_e contains losses from the RF couplers, radiation losses and conduction losses on the main mirror. Q_{rw} is due to losses of the coated probe mirror and is inversely proportional to its surface resistivity:

$$Q_{rw} = \frac{C}{R_s},$$

where $R_s = \Re(Z_s)$ is related to the coating thickness d via the well-known transmission line equation:

$$Z_s = Z_{NEG} \frac{(Z_{NEG} + Z_{Cu}) - (Z_{NEG} - Z_{Cu})\ e^{2ik_{NEG}d}}{(Z_{NEG} + Z_{Cu}) + (Z_{NEG} - Z_{Cu})\ e^{2ik_{NEG}d}}$$

The unknowns C and Q_e are obtained by measuring uncoated calibration probes with known properties, manufactured from stainless steel ($\kappa = 1.45 \cdot 10^6$ Sm) and copper ($\kappa = 5.8 \cdot 10^7$ Sm).

$$Z_{NEG} = \sqrt{\frac{i\omega\mu}{\sigma_{NEG}}}\ ,\ Z_{Cu} = \sqrt{\frac{i\omega\mu}{\sigma_{Cu}}}\ ,\ k_{NEG} = \sqrt{i\omega\mu\sigma_{NEG}} \tag{2}$$

Table 2: Coating thickness and total Q for all samples including copper and stainless steel references.

	d_{avg}/nm	81 GHz	102 GHz	163 GHz
Cu	N/A	26567	15552	28184
SS	N/A	16951	11975	14606
NEG1	788	24753	14829	21575
NEG2	696	24753	14770	20924
NEG3	735	25075	14805	21244
NEG4	661	25729	15256	22712

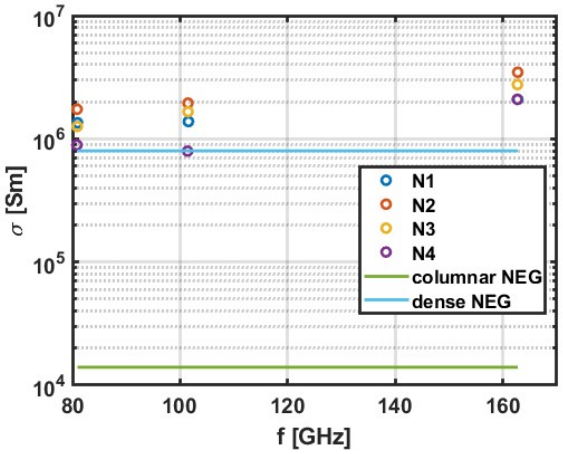

Figure 5: Estimated bulk conductivity of the NEG coatings, indicated also the nominal values for columnar and dense NEG.

Using the two test stands, we performed measurements at 81,102 and 163 GHz, frequencies where we found usable resonances. A set of four samples were coated at PSI and measured in terms of thickness, Table 2 shows the results as well as the quality factors and includes results measured for the calibration samples fabricated from stainless steel (SS) and copper (Cu). The calibration measurements define a relationship between coating thickness, NEG conductivity and the expected quality factor. For evaluating the quality of the measurements, one has to keep in mind that the coating thickness of the samples were not perfectly flat, but shows variations in the order of 100–200 nm.

Fixing the thickness to the values of Table 2, we arrive at the estimated conductivities in Fig. 5. This kind of fit is more sensitive to input variations, so the conductivities deviate quite a bit from the nominal one. Nonetheless, it allows a clear indication of the morphology of coating as dense.

Fitting becomes quite a bit easier, if we use it to determine coating thickness. If we fix the conductivity to the nominal value of dense NEG of $8 \cdot 10^5$ Sm, we arrive at the results shown in Fig. 6. The difference between the electrical and mechanical thickness is typically in the order of 10% (70 nm) and below 30% (200 nm), which is excellent given the irregularities mentioned above.

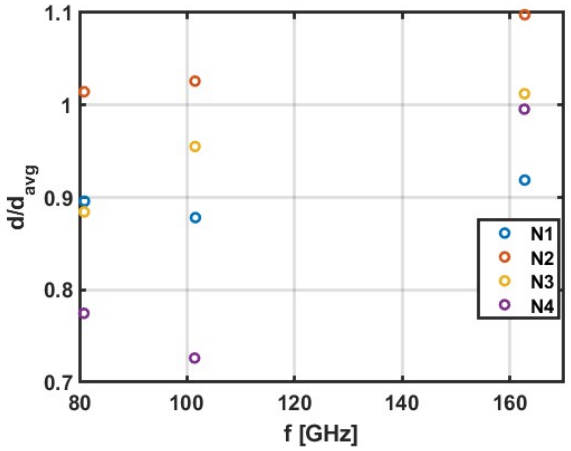

Figure 6: Estimated thickness of the NEG coatings normalized to the average thickness, assuming the conductivity of dense NEG.

SUMMARY AND OUTLOOK

Non evaporable getters coatings help to solve problems related to multipactor, electron and photon stimulated desorption and for integrated pumping for vacuum devices. In high intensity electron storage ring, their low conductivity require a defined morphology and ultra thin coating thickness to avoid excessive resistive wake fields. To characterize very thin coatings, we designed and built two quasi-optical test systems. These consist of a half symmetric Fabry-Perot resonator, which is able to measure compact planar samples compatible in the 100 and 170 GHz range. The measurements allow to prove the morphology of the coating and give a good accuracy in measuring the thickness.

REFERENCES

[1] C. Benvenuti, "Non-evaporable getters; from pumping strips to thin film coatings", in *Proc EPAC'98*, Stockholm, Sweden, Jun. 1998, paper THZ02A, pp. 200–206.

[2] B. Henrist *et al.*, "The secondary electron yield of TiZr and TiZrV non evaporable getter thin film coatings", CERN, Geneva, Switzerland, Rep. CERN-EST 2000-07(SM), 2000.

[3] O. B. Malyshev *et al.*, "Activation and measurement of nonevaporable getter films", Journal of Vacuum Science and Technology A, vol. 27, p. 321, 2009. doi:10.1116/1.3081969

[4] SLS 2.0 Storage Ring Technical Design Report, PSI, Villigen, Switzerland, Rep. 21-02, November 2021.

[5] A. Streun *et al.*, "SLS-2- the upgrade of the Swiss Light Source", *J. Synchrotron Radiat.*, vol. 25, p. 631, 2018. doi:10.1107/S1600577518002722

[6] M. Dehler *et al.*, "Conceptual Design for SLS-2", in *Proc. FLS'18*, Shanghai, China, Mar. 2018, pp. 150-153. doi:10.18429/JACoW-FLS2018-WEP2PT038

[7] O. B. Malyshev *et al.*, "RF surface resistance study of nonevaporable getter coatings", *Nucl. Instrum. Methods*, vol. 844, p. 99, 2017. doi:10.1016/j.nima.2016.11.039

[8] E. Koukovini-Platia *et al.*, "Electromagnetic characterization of nonevaporable getter properties between 220–330 and 500–750 GHz for the Compact Linear Collider damping rings", *Phys. Rev. Accel. Beams*, vol. 20, p. 011002, 2017. doi:10.1103/PhysRevAccelBeams.20.011002

[9] M. Dehler *et al.*, "Characterization of NEG Coatings for SLS 2.0", in *Proc. IPAC'19*, Melbourne, Australia, May 2019, pp. 1662-1665. doi:10.18429/JACoW-IPAC2019-TUPGW108

[10] J. R. Kessler, J. M. Gering, and P. D. Coleman, "Use of a Fabry-Perot Resonator for the measurement of the surface resistance of high Tc superconductors at millimeter wave frequencies", *Int. J. Infrared Millimeter Waves*, vol. 11, p. 151, 1990. doi:10.1007/BF01010512

[11] S. J. Hogen, "Use of a Fabry-Perot resonator at millimeter wave frequencies in the determination of thin-film resistivities", Technical Rep. SERI/TR-32-227, Solar Energy Research Inst., National Renewable Energy Lab. (NREL), Golden, CO, USA, Aug. 1979. doi:10.2172/5927333